HHS Public Access

Author manuscript

J Thromb Haemost. Author manuscript; available in PMC 2022 January 01.

Published in final edited form as:

J Thromb Haemost. 2021 January ; 19(1): 161–172. doi:10.1111/jth.15115.

Thrombin-PAR1 signaling in pancreatic cancer promotes an immunosuppressive microenvironment

Patrick G. Schweickert[1], **Yi Yang**[2], **Emily E. White**[1], **Gregory M. Cresswell**[3], **Bennett D. Elzey**[3], **Timothy L. Ratliff**[3], **Paritha Arumugam**[4], **Silvio Antoniak**[2], **Nigel Mackman**[5], **Matthew J. Flick**[2,*], **Stephen F. Konieczny**[1]

[1]Purdue University, Department of Biological Sciences and the Purdue Center for Cancer Research, West Lafayette, Indiana, USA

[2]University of North Carolina, Department of Pathology and Laboratory Medicine, the Lineberger Comprehensive Cancer Center, and the UNC Blood Research Center, Chapel Hill, North Carolina, USA

[3]Purdue University, Department of Comparative Pathobiology and the Purdue Center for Cancer Research, West Lafayette, Indiana, USA

[4]Cincinnati Children's Hospital Medical Center, Division of Pulmonary Biology, Cincinnati, Ohio, USA

[5]University of North Carolina, Department of Medicine and the UNC Blood Research Center, Chapel Hill, North Carolina, USA

Abstract

Background: Pancreatic ductal adenocarcinoma (PDAC) is characterized by a prothrombotic state and a lack of host anti-tumor immune responsiveness. Linking these two key features, we previously demonstrated that tumor-derived coagulation activity promotes immune evasion. Specifically, thrombin-protease-activated receptor-1 (PAR1) signaling in mouse PDAC cells drives tumor growth by evading cytotoxic $CD8a^+$ cells.

Methods: Syngeneic mixed cell tumor growth, transcriptional analyses, and functional tests of immunosuppressive response genes were employed to identify cellular and molecular immune evasion mechanisms mediated by thrombin-PAR-1 signaling in mouse PDAC tumor cells.

[*]**Correspondence:** Matthew J. Flick, Associate Professor, University of North Carolina at Chapel Hill, Department of Pathology and Laboratory Medicine, Lineberger Comprehensive Cancer Center, UNC Blood Research Center, 116 Manning Drive, Office 8018B, Chapel Hill, NC 27599, Phone: 919-843-1339 matthew_flick@med.unc.edu.

Author Contributions

Study conception and experimental designs were carried out by PGS, YY, SFK and MJF with additional consultation from BDE and GMC. PGS, EW, SFK and YY carried out experiments, collected data, and analyzed the results and BDE, GMC, TLR, SA, NM and PA provided needed reagents. The manuscript was written by PGS, YY, SFK and MJF. All authors reviewed the final version of the manuscript.

Conflict of Interest

The authors declare that the research was conducted in the absence of any commercial or financial relationships that could be construed as a potential conflict of interest.

Data availability statement

The datasets analyzed for this study can be found in the Gene Expression Omnibus https://www.ncbi.nlm.nih.gov/geo/query/acc.cgi?acc=GSE120370.

Results: Elimination of tumor cell PAR1 in syngeneic graft studies increased cytotoxic T lymphocyte (CTL) infiltration and decreased tumor-associated macrophages in the tumor microenvironment. Co-injection of PAR1-expressing and PAR1-knockout (PAR-1^{KO}) tumor cells into immunocompetent mice resulted in preferential elimination of PAR-1^{KO} cells from developing tumors, suggesting that PAR1-dependent immune evasion is not reliant on CTL exclusion. Transcriptomics analyses revealed no PAR1-dependent changes in the expression of immune checkpoint proteins and no difference in MHC-I cell surface expression. Importantly, thrombin-PAR1 signaling in PDAC cells upregulated genes linked to immunosuppression, including *Csf2* and *Ptgs2*. Functional analyses confirmed that both *Csf2* and *Ptgs2* are critical for PDAC syngeneic graft tumor growth and overexpression of each factor partially restored tumor growth of $PAR1^{KO}$ cells in immunocompetent mice.

Conclusions: Our results provide novel insight into the mechanisms of a previously unrecognized pathway coupling coagulation to PDAC immune evasion by identifying PAR1-dependent changes in the tumor microenvironment, a PAR1-driven immunosuppressive gene signature, and *Csf2* and *Ptgs2* as critical PAR1 downstream targets.

Keywords

pancreatic ductal adenocarcinoma; immune evasion; immunosuppression; cancer; protease activated receptor 1; thrombin; cytotoxic T lymphocyte

Introduction

Pancreatic ductal adenocarcinoma (PDAC) is a highly fatal malignancy with an average 5-year rate of survival estimated at 8% [1]. This poor prognosis can be largely attributed to two distinguishing features of the disease. First, PDAC is associated with dysregulation and hyperactivation of the coagulation system. Consequently PDAC poses the highest risk for venous thromboembolism compared to other cancer types [2–4]. Indeed, cancer-associated thromboembolism accounts for the second leading cause of cancer related deaths [2]. Secondly, PDAC is a poorly immune responsive disease [5–7]. While the development of immune checkpoint inhibitors as therapeutics has been an important breakthrough in the treatment of a number of solid and hematological cancers, they have been ineffective as a PDAC therapy, likely due to the non-immunogenic nature of the disease and the frequent lack of infiltrating cytotoxic T cells [8]. These two prominent pathological features of PDAC have historically been viewed as distinct, but recent data suggests they may be highly integrated, although precise mechanisms of crosstalk remain undefined.

In addition to increasing the prevalence of thromboembolic events, pathological activation of the coagulation pathway can also promote cancer progression (reviewed in ref [9]). Protease activated receptor-1 (PAR1) is a direct downstream effector of the central coagulation protease thrombin. PAR1 is a seven transmembrane G protein-coupled receptor uniquely and irreversibly activated following proteolytic cleavage of its amino-terminal region resulting in the creation of a tethered ligand that can bind and activate the receptor (reviewed in ref [10]). Through expression on a wide range of cell types, PAR1 signaling can impact a number of cellular and tissue processes, including tissue remodeling, inflammation, endothelial barrier function, and fibrosis among other cellular effector functions [11–13]. In regard to cancer

progression, studies have shown that functional roles of PAR1 signaling are highly cancer cell-type specific [9,14,15]. The majority of findings indicate that PAR1 enhances tumorigenesis, proliferation, migration, and metastasis across multiple tumor models [16–21]. Most of these studies have centered on defining possible tumor cell autonomous effects of PAR1 signaling using cell lines transplanted in immunocompromised animals, potentially missing the connections between PAR1 signaling and tumor immunity. Through the use of a syngeneic mouse PDAC tumor model, our group for the first time identified a novel but previously undefined mechanism of tumor cell thrombin-PAR1 signaling that promotes PDAC progression through evasion of anti-tumor immunity [22].

In this study, cellular and molecular PAR1-driven changes in the PDAC tumor inflammatory microenvironment were investigated. The transcriptional landscape indicated that loss of PAR1 causes an increase in the anti-tumor inflammatory response, rendering PDAC cells susceptible to targeted elimination by the immune system. Furthermore, thrombin-PAR1 downstream immune response genes, including *Ptgs2* and *Csf2*, were identified as critical factors in PDAC tumorigenesis whose overexpression is capable of restoring tumor growth, even in the absence of PAR1.

Materials and Methods

Cell culture

LSL-KRas^{G12D}, *LSL-Trp53*^{R172H}, *Elastase*$_{pr}^{CreER}$ (KPC) PAR1 expressing and PAR1^{KO} cell lines have been described and characterized previously [22]. To generate eGFP and tdTomato expressing stable cell lines, lentiviral vectors were produced in 293T cells using a four plasmid transfection system by a calcium chloride and 2X HBS precipitation method. Briefly, transfections were carried out using 8 μg of third-generation lentiviral vector plasmids LeGO-T2 (Addgene) or LeGO-G2 (Addgene) [23]. KPC cells were transduced with serially diluted concentrated virus and transduced pooled cells with a high percentage of vector expression were sorted for either eGFP or tdTomato positive cells using a BD FACS Aria II cell sorter system to generate the final KPC-eGFP+ or KPC-tdTomato+ cell lines. PAR1^{KO} “rescue” cell lines were generated using lentiviral particles from VectorBuilder and included a CMV-EGFP:T2A:Puro-EF1A-mCherry vector as a control. Pooled cell lines were selected using 250 μg/mL Geneticin G418 (Gibco). Alternatively, FACS was used based on mCherry expression for the control expression vector. Transduced cell lines were assessed by RT-qPCR and then used for subsequent experiments. For cell stimulation experiments, cell were cells were first serum starved in 1% FBS containing media overnight and then treated with thrombin (1 U/mL; Enzyme Research Lab), activated protein C (500 nM; Hemtologic Technologies), plasmin (300 nM; Hematologic Technologies) or vehicle for 24 hours followed by the addition of 20 ng/mL recombinant IFNγ (cat # 575302, BioLegend) for 24 hours before cells were harvested for analysis.

Genetic deletion of *Csf2* and *Ptgs2* expression was achieved using a modified CRISPR/Cas9 system [24]. The details of the gene editing are provided in the supplemental methods. The presence of insertions or deletions was detected by PCR and polyacrylamide gel electrophoresis, as described elsewhere (see [25]). Results were confirmed by ELISA for GM-CSF (R&D Systems), and PGE_2 (Cayman Chemical).

Syngeneic graft tumor studies

Syngeneic graft studies were performed using 8–12 week-old wild type C57BL/6 mice or PAR-1$^{-/-}$ mice [26]. Cells were dissociated by trypsin, washed once in media followed by sterile PBS, and finally resuspended in ice cold sterile PBS prior to injection. Anesthetized mice were injected subcutaneously with 5×10^5 cells per animal in 200 μl PBS. Tumor volume was measured every 2–4 days using calipers, as described previously [22]. For lymphocyte depletion, intraperitoneal injections of monoclonal antibodies targeting CD8a (clone 2.43) were performed. Antibodies were harvested and purified in house. Dosages for injection were determined in separate titration experiments. Mice were injected twice weekly starting one day prior to tumor cell injection.

Tumor dissociation and flow cytometry

The tumor dissociation protocol was adapted and modified from Pasut et al. (2012) [27]. Briefly, tumors between 10–100 mm^3 were excised, placed in ice cold PBS, finely minced with a razor blade, and resuspended in 1 mL digestion buffer in PBS containing 2 U/mL Collagenase B (Roche), 2 U/mL Dispase II in 10 mM NaAc (pH 7.5), 5 mM CaAC buffer (Sigma), 50 mM HEPES pH 7.4, 150 mM NaCl, and 1 μg/mL DNase I. The tissue was incubated at 37 °C for 45 minutes or until samples were well digested. A solution of 20% FBS in PBS was added and samples were passed through a 70 μm filter. Cells were collected by centrifugation. Pellets were resuspended in 500 μl red blood cell lysis buffer at room temperature for 2 minutes. Samples were treated with 3 ml of 10% FBS and passed through a 40 μm filter and collected by centrifugation. Pellets were resuspended in MACS buffer (1 mM EDTA, 2% FBS in PBS) for staining. Following an Fc block, cells were stained for 30 minutes on ice and protected from light with fluorescently-conjugated antibodies at 1:400 dilution each and a 1:1000 dilution of live/dead stain (Thermo Scientific, Waltham, MA). See supplemental materials and methods for antibodies used for analysis. Cells were analyzed on a BD LSRFortessa flow cytometer. Compensation controls were set using UltraComp eBeads (Thermo Scientific). Final analysis was performed using FlowJo.

Immunofluorescence staining

Tumor samples were fixed in 10% neutral buffered formalin, processed and dehydrated, embedded in paraffin blocks, and mounted on glass slides. Slides were deparaffinized, permeabilized with 0.1% triton X-100 in PBS for 20 minutes, and treated with blocking solution (Vector Laboratories) containing 4 drops/mL of an avidin blocking reagent (Vector Laboratories). Staining was performed with primary antibodies including, anti-GFP (cat# ab13970, Abcam) and anti-RFP (Rockland), which were prepared at dilutions of 1:300 each in a staining diluent (Vector Laboratories) in conjunction with secondary antibody (1:200), goat anti-rabbit biotin (Vector Laboratories), and detection with avidin alexa 594 (Thermo Scientific), 488-goat anti-chicken (Invitrogen), and 1:500 dilution of DAPI. Images were captured using an Olympus BX51 microscope with an Olympus DP80 camera and CellSense Entry software.

RNA extraction, RT-qPCR analysis, and RNA-Seq

Relative expression was then determined using the ΔΔCt method. RNA-Seq results and the corresponding experimental design were described previously [22] and represent transcriptional changes induced by thrombin after 24 hours *in vitro*. The full dataset can be found on the GEO database accession number GSE120370. Additional detailed information may be found in the Supplementary Material.

Patient Survival Analysis

Patient survival and transcriptomics data were obtained from The Cancer Genome Atlas (TCGA) and low and high gene expression was stratified to obtain the most significant separation between groups as obtained from the human protein atlas' [28] TCGA survival analysis.

Statistical analysis

Results were analyzed using unpaired Student's t-test with Welches' correction applied where applicable. For multiple comparisons a one-way ANOVA followed by Tukey's or Dunnett's post hoc test was used as indicated. Subcutaneous tumor growth studies were analyzed using repeated measures ANOVA. All statistical analysis was performed using GraphPad Prism (v8.3).

Ethical approval

All animal studies were carried out following the guidelines and approval of the Purdue University or University of North Carolina Animal Care and Use Committee under protocols 1110000037 and 19-204, respectively. All efforts were made to minimize animal suffering.

Results

PAR1 expression influences the tumor immune response and impacts PDAC cell susceptibility to immune cell-mediated elimination.

PAR1 expression by murine *LSL-KRas*^{G12D}, *LSL-Trp53*^{R172H}, *Elastase*$_{pr}$^{CreER} (KPC) PDAC cells was previously shown to significantly enhance tumor growth in immunocompetent mice by supporting evasion of anti-tumor immunity [22]. Consistent with our earlier findings, KPC-PAR1^{KO} cells formed small tumors when subcutaneously injected into syngeneic wildtype (WT) C57BL/6 mice, but most tumors began to regress within 9–10 days, matching a pattern consistent with an adaptive anti-tumor immune response (Figure 1A). Accordingly, PAR1^{KO} tumor growth could be partially restored by CD8a^{+} cell depletion (Figure 1A). To gain mechanistic insight into the differences between PAR1 expressing KPC (PAR1^{WT}) and PAR1^{KO} PDAC tumors, flow cytometry was used to analyze the infiltrating immune cell populations (Figure 1B). A dramatic and significant increase in the presence of CD8a^{+} T cells in the PAR1^{KO} tumors was observed, in agreement with the finding that these tumors are subject to elimination through a CD8a^{+} driven immune response. No difference in the presence of CD4 T cells was detected and our previous study showed that depletion of this cell population had no impact on PAR1^{KO} tumor growth [22]. In contrast, PAR1^{KO} tumors showed decreased levels of immune cell populations capable of

exerting protumorigenic and immunosuppressive functions, including tumor-associated macrophages (TAMs) [29] as well as granulocytic-myeloid-derived suppressor cells (G-MDSCs) [30]. Analysis of KPC ($PAR1^{WT}$) tumor growth in C57BL/6 WT or $PAR1^{-/-}$ mice revealed no difference in tumor growth, similar to as we have demonstrated previously (Supplement Figure 1A, 1B and see [22]). RT-qPCR analysis of immune cell markers within tumor tissue revealed no difference in the macrophage markers *Adgre1* (F480) and *Cd68* nor in the T cell markers *Cd3e* and *Cd4* (Supplement Figure 1C–1F). A modest, albeit statistically significant increase in *Cd8a* was observed (Supplement Figure 1G). Thus, tumor cell PAR1 expression fosters a cellular microenvironment within tumors characterized by low levels of cytotoxic T cell infiltration and increased protumorigenic and immunosuppressive cell types. Conversely, loss of tumor cell PAR1 promotes the formation of an anti-tumor proinflammatory immune profile, whereas loss of stromal cell PAR1 makes little to no contribution to the immune profile in this model.

Tumor immune cell profiles suggested PAR1 was functioning by preventing the accumulation of tumor targeting immune cells in the tumor microenvironment. To determine if this was a dominant and systemic effect transferable to neighboring cells, we tested whether $PAR1^{WT}$ cells could provide protection for $PAR1^{KO}$ cells when both cell lines were mixed and co-injected into C57BL/6 mice. In order to properly assess the proportion of $PAR1^{WT}$ to $PAR1^{KO}$ cells in the resulting tumors, both cell lines were transduced with lentiviral vectors expressing eGFP or tdTomato as outlined in Figure 1C. Tumors were then harvested and analyzed by flow cytometry at 5- and 25-days post-injection. Whereas within 5 days of injection tumors consisted of roughly equal proportions of $PAR1^{WT}$ and $PAR1^{KO}$ cells, at day 25 $PAR1^{KO}$ tumor cells were almost completely eradicated from mice challenged with a mixed cell population (Figure 1D, 1E). This finding suggested that $PAR1^{WT}$ PDAC cells did not exert a local positive influence on the tumor growth of the $PAR1^{KO}$ cells. Notably, similar to our earlier findings, $PAR1^{KO}$ tumor cell growth within the mixed tumors could be partially restored by depletion of $CD8a^{+}$ cells (Figure 1F), indicating that a $CD8a^{+}$ cell dependent anti-tumor immune reaction was still taking place within the mixed tumor environment. These results indicate that PAR1 expression does not protect tumor cells through a dominant systemic reshaping of the tumor microenvironment or through a T cell exclusion mechanism, as $PAR1^{KO}$ tumor cells were still eliminated from the mixed tumors by an adaptive immune response. Rather, these data indicate that $PAR1^{KO}$ tumor cells are preferentially targeted and eliminated and are therefore more readily detected by and/or susceptible to infiltrating immune cells compared to PAR1 expressing PDAC cells.

Syngeneic graft tumor re-challenge experiments were next performed to further elucidate how $PAR1^{WT}$ PDAC cells are protected from the anti-$PAR1^{KO}$ tumor cell immune response. For these studies two strategies for re-challenge were employed. $PAR1^{KO}$ tumor cells were injected subcutaneously into the intrascapular region of C57BL/6 mice and allowed to be fully cleared by the immune system prior to injecting $PAR1^{WT}$ cells into (*i*) the flank or (*ii*) the original intrascapular injection site (Figure 1G, 1H). In both instances, previous exposure and clearance of $PAR1^{KO}$ tumors offered no protection against the $PAR1^{WT}$ re-challenge. Collectively, the mixed tumor cell and tumor re-challenge results indicate that $PAR1^{WT}$ cells do not rely on the exclusion of anti-tumor immune cells as a primary means of immune

evasion, but rather PAR1 renders PDAC cells either undetectable and/or less susceptible to immune cell-mediated elimination.

Thrombin-PAR1 signaling decreases the expression of antigen processing machinery genes but does not alter MHC-I or PDL-1 cell surface expression.

CD8a$^+$ cytotoxic T lymphocytes recognize target cells through the interaction of their T cell receptor with antigen presenting major histocompatibility complex class I (MHC-I) molecules on the surface of the target cell. Cancer cells can avoid detection, and thus elimination, through loss of MHC-I expression [31]. Accordingly, a PAR1-dependent decrease in MHC-I presentation could result in escape of PAR1^{WT} cells from elimination while simultaneously allowing neighboring PAR1^{KO} cells to be targeted and killed. Analysis of RNA-Seq data to determine transcriptional changes induced by PAR1 signaling *in vitro* (GSE120370) revealed no changes in the expression of MHC-I genes upon PAR1 activation (data not shown). However, *Tap1*, which encodes an ABC transporter essential for MHC-I antigen loading, was significantly downregulated by PAR1 signaling, as were several other genes within or related to the antigen processing and MHC-I peptide loading pathway including upstream IFNγ receptors (*Ifngr1, Ifngr2*), the immunoproteasome peptidase gene *Psbm8*, *Tap1* associated peptide loading genes (*Tapbp*, *Tapbpl*), as well as the ER chaperone *Calr*, while *Prdm1*, which encodes a transcription factor known to negatively regulate MHC-I loading genes [32], was upregulated (Figure 2A). Since MHC-I stability and cell surface occupancy is dependent on the proper expression and function of these genes [31,33], we performed flow cytometry to determine whether PAR1 activation caused changes in MHC-I protein levels on the cell surface. Importantly, MHC-I protein was detectable at similar levels in PAR1^{KO} and PAR1^{WT} cells (Figure 2B, 2C). Treatment of the PAR1^{WT} cells with thrombin had no impact on MHC-I cell surface expression. In addition, thrombin stimulation did not alter IFNγ-mediated upregulation of MHC-I cell surface expression. We next analyzed the impact of PAR1 on tumor cell MHC-I *in vivo*. Mice were injected subcutaneously with either PAR1^{WT} or PAR1^{KO} fluorescently labeled tdTomato expressing tumor cells an to properly identify the tumor cell population by flow cytometry. Tumor samples were harvested 7-days post injection when tumors were still detectable in both groups. Similar to our *in vitro* studies, flow cytometry analysis showed equal expression of the MHC-I protein H-2Kb in both the PAR1^{WT} and PAR1^{KO} isolated tumor cells (Figure 2D, 2E). Notably, the we also observed no differences in MHC-I cell surface expression following KPC cell stimulation with activated protein C or plasmin (Supplement Figure 2) Consequently, while it appears that PAR1 activation broadly impacts the transcription of genes related to antigen processing and MHC-I loading, this affect does not translate to a detectable decrease in MHC-I cell surface localization.

Tumor cells can also avoid immune clearance by activating inhibitory checkpoint proteins on immune cells. The programmed cell death receptor (PD1) is one of the best studied of these immune inhibitory receptors and is the target of several FDA approved cancer therapeutics [34]. Therefore, we determined whether PAR1 activation had any influence on the expression of PDL1, the PD1 ligand. Despite the importance of PDL1 to immune evasion we detected no change in PDL1 gene expression within the RNA-Seq dataset (Figure 2F). Further, flow cytometry analysis confirmed that PDL1 protein expression was similar

between PAR1^{KO} and PAR1^{WT} cells and unaltered by PAR1 activation, although as with MHC-I expression, PDL1 was increased by IFNγ stimulation (Figure 2G, 2H).

PAR1 signaling induces an immunosuppressive gene signature.

To more broadly interrogate downstream effectors of the thrombin-PAR1 signaling pathway that could promote tumor immune evasion, the RNA-Seq dataset was queried to identify genes associated with other immune pathways including known inhibitory checkpoint ligands, genes involved in adenosine metabolism, and genes associated with immunosuppression (Figure 3A). This assessment identified a signature of nine genes (*Ido1, Ido2, Fas, Ccl2, Ptgs2, Csf2, Siglec15, Il34*, and *Tgfb1*) that were differentially expressed following PAR1 activation and that could contribute to tumor immune evasion based on their pattern of expression [35,36,45,46,37–44]. To confirm that PAR1 altered the expression of these genes *in vivo*, RT-qPCR was performed using mRNA from PAR1^{KO} and PAR1^{WT} tumors. CD8a^{+} cell depleted PAR1^{KO} tumor samples were also analyzed to determine whether differences in gene expression were due to the presence or absence of tumor-derived PAR1 or a result of disparities in tumor size and the level of cytotoxic T cell infiltration (Figure 3B). *Ido1* and *Ido2* were actually expressed at higher levels in the PAR1^{KO} tumors, though whether this was due to increased expression by the tumor cells or by other cells within the tumor milieu remains to be determined (Figure 3C, 3D). Additionally, expression of *Fas* and *Ccl2* were unaffected by the status of PAR1 (Figure 3E, 3F). However, the remaining five genes (*Ptgs2, Csf2, Siglec15, Il34, Tgfb1*) showed significant PAR1-dependent upregulation both *in vitro*, based on the RNA-Seq results (Figure 3A), and *in vivo* (Figure 3G– 3K), thus representing a potential PAR1-driven immunosuppressive gene signature.

Ptgs2 and *Csf2* can restore tumor growth in the absence of PAR1 and are critical for PDAC tumor growth.

To determine if expression of any of the immunosuppressive genes identified above could restore PAR1^{KO} tumor growth, and therefore compensate for the loss of PAR1, stable cell lines were generated by viral transduction to “rescue” target gene expression (Figure 4A, 4B). Tumor growth was then assessed in immunocompetent C57BL/6 mice. While most genes had no significant influence on PAR1^{KO} tumor growth, both *Csf2*, encoding GM-CSF, and *Ptgs2*, which encodes COX2, independently restored the tumor forming capacity of PAR1^{KO} cells to varying degrees (Figure 4C). Notably, ectopic expression of *Csf2* had a dramatic effect, resulting in strikingly expedited tumor growth but also severe splenomegaly, areas of pulmonary hemorrhage identifiable at both the macroscopic and microscopic level (data not shown), and increased animal frailty, requiring early termination of the *Csf2*-expressing cohort. Similar GM-CSF-dependent phenotypes have been reported where GM-CSF has been shown to play a role in acute pancreatitis-associated lung injury [47] and in tissue wasting [48].

Analysis of survival data from the cancer genome atlas (TCGA) revealed that PDAC patients with low expression of PTGS2 or CSF2 had significantly improved survival (Figure 4D, 4G). Given these findings, the importance of *Ptgs2* and *Csf2* for tumor growth in PAR1 expressing control KPC cells was next assessed. KPC *Ptgs2* and *Csf2* knockout cell lines

were generated using an established gene editing system [24]. ELISA analyses confirmed that GM-CSF and PGE_2 secretion was eliminated in the knockout lines but was indeed increased in control cells upon PAR1 activation by thrombin (Figure 4E, 4H). Syngeneic graft experiments using the newly generated knockout KPC lines revealed that ablation of *Csf2* or *Ptgs2* greatly attenuated tumor growth in C57BL/6 mice (Figure 4F, 4I) where 3 out of 3 $Ptgs2^{KO}$ lines and 3 out of 4 $Csf2^{KO}$ lines failed to produce significant tumors, despite maintaining the $KRas^{G12D}$ and $Trp53^{R172H}$ driver mutations. These results show that *Csf2* and *Ptgs2* display a PAR1-dependent expression pattern and are critical for PDAC tumorigenesis. Importantly, both factors promote tumor growth in $PAR1^{KO}$ PDAC cells, thus compensating for the absence of PAR1 and identifying a previously underappreciated association between PAR1, *Csf2, Ptgs2*, and tumor immune evasion.

Discussion

A robust procoagulant phenotype and resistance to anti-tumor immunity are two dominant characteristics of PDAC. Although these two features have historically been viewed as separate and distinct, our data suggest they are highly integrated functional pathways. The results presented here extend our previous findings and provide cellular and molecular mechanistic details into the role of thrombin-PAR1 signaling in PDAC immune evasion. Analysis of tumor immune cell infiltrates revealed that $PAR1^{WT}$ tumors contained a drastically smaller population of CD8 T cells compared to $PAR1^{KO}$ samples. This finding was consistent with an initial hypothesis that PAR1 expression promotes T cell exclusion and the establishment of a myeloid cell dominated immunosuppressive tumor microenvironment, thereby protecting PDAC cells through a mechanism of immune privilege. Such a mechanism is consistent with previous reports using PDAC mouse models where cytotoxic T cells were rarely present during spontaneous PDAC tumor development and were similarly unresponsive in syngeneic graft experiments [5,6]. However, the $PAR1^{KO}$/$PAR1^{WT}$ mixed cell tumor study revealed that functional anti-tumor cytotoxic T cells were present and active in the tumor microenvironment at a level capable of eliminating the $PAR1^{KO}$ PDAC cells while leaving $PAR1^{WT}$ cells free to proliferate. $PAR1^{WT}$ cells do show an increase in tumor growth following CD8 T cell depletion [22], suggesting that even though the level of infiltrating CD8 T cells is low in $PAR1^{WT}$ tumors, $PAR1^{WT}$ cells are still targeted by an adaptive immune response, albeit one that $PAR1^{WT}$ cells can readily overcome. This finding also implies that some degree of T cell priming occurs in PAR1 expressing tumors. Nevertheless, our studies indicate that PAR1 expression on PDAC cells does not promote immune evasion by generating an immune privileged microenvironment.

The concept that PAR1 expressing PDAC cells are protected from an active intratumoral immune response was further supported by the finding that previous exposure and clearance of $PAR1^{KO}$ tumors offered no protection against $PAR1^{WT}$ tumor growth in C57BL/6 mice. Although both PDAC cell lines share the same origin, it is unknown whether the two lines share common antigens. It is possible that the presence or absence of PAR1 signaling in KPC PDAC changes the repertoire of tumor cell antigens that cytotoxic T cells may encounter. Given that mice that previously encountered and eliminated KPC $PAR1^{KO}$ cells through an adaptive immune response were unable to mount a similar immune reaction

against KPC PAR1^{WT} cells when rechallenged, the antigens could be distinct. Similar to the PAR1^{KO}/PAR1^{WT} mixed cell tumor study these results support the conclusion that PAR1-expression renders PDAC cells less susceptible to elimination, even in animals primed and ready to target KPC tumor cells. Of note, we previously demonstrated that re-expression of a PAR1 transgene in the PAR1^{KO} cells completely restores tumor growth to PAR1^{WT} levels [22]. Thus, the presence or absence of PAR1 is the critical factor in this system. Whether and how PAR1 expression and signaling changes the composition of tumor cell antigens, either positively or negatively, will be a focus of future investigations.

To start to identify mechanisms of thrombin-PAR1-driven PDAC immune evasion we utilized RNA-Seq data reflecting transcriptional changes induced by PAR1 signaling *in vitro* to look for gene expression patterns that could explain our results. Interestingly, PAR1 activation had a broad impact on genes related to antigen processing and loading machinery, markedly causing a significant > 2-fold decrease in *Tap1*, while other genes showed a general trend of having decreased expression. Ultimately, this downregulation did not translate to a quantitative difference in cell surface occupancy of MHC-I. Nevertheless, it remains interesting and curious that PAR1 would influence so many genes within this pathway. Similarly, expression of PDL1, another key factor that is tightly linked to elimination of tumor cells by the host immune system remained unaffected by PAR1. Notably, the IFNγ receptor subunit *Ifngr2* was also significantly decreased by PAR1 signaling, although again this did not influence the effects of IFNγ on either MHC-I or PDL-I induction.

An extensive analysis of the RNA-Seq also showed no evidence that immune inhibitory checkpoint ligands (*e.g., Cd80, Vsir, Vtcn1*) were upregulated by PAR1 nor were there signs of an increase in adenosine metabolism. Surprisingly, some well characterized PAR1 downstream targets related to inflammation were also unresponsive or even downregulated in our analysis, including *Il6, Cxcl1, Cxcl2, Cxcl5, Vcam1*, and *Icam1* [11], suggesting that thrombin-PAR-1 signaling can exert cell type specific effects. However, these studies did identify an immunosuppressive PAR1-mediated gene signature, which included several genes previously linked to thrombin signaling, namely *Fas* [49], *Ccl2* [50,51], *Ptgs2* [52–54], *Csf2* [55,56], and *Tgfb1* [57]. Of the downstream targets identified, *Ptgs2, Csf2, Siglec15, Il34*, and *Tgfb1* also showed PAR1-dependent expression patterns *in vivo*. The precise reasons for the discrepancy in gene expression patterns between the *in vitro* RNA-Seq and *in vivo* tumor data require further analysis. A possible explanation is likely linked to the complexity of the *in vivo* tumor microenvironment. Various stromal cell types (*e.g.*, immune cells, fibroblasts, endothelial cells), extracellular matrix components, and secreted soluble molecules could each exert a profound influence on tumor cell behavior through mechanisms both dependent and independent of tumor cell PAR1 signaling [58]. Notably, however, stromal PAR1 did not influence KPC tumor growth based on our syngeneic tumor studies using PAR1 −/− mice. Within the immunosuppressive PAR1-regulated gene signature both *Csf2* and *Ptgs2* have previously been identified as critical mediators of PDAC immunosuppression and immune evasion [39–41]. In agreement with these results we found that ablation of *Csf2* or *Ptgs2* to be largely detrimental to PDAC tumor growth. Importantly, when ectopically expressed in PAR1^{KO} cells *Csf2* and *Ptgs2* independently restored tumor growth, thus overcoming the deficiencies in immune evasion created by the absence of

PAR1. *Csf2* and *Ptgs2* therefore represent two factors regulated by PAR1-signaling with demonstrably critical roles in PDAC tumor growth and immune evasion.

It is important to note that the studies presented here are predicated on the concept that the activator of tumor cell PAR1 is thrombin. Whereas our present and previous data [22] are consistent with the thrombin-PAR1 pathway playing an active role, it is possible that other PAR1 agonists may also contribute to PDAC pathogenesis. PAR1 activators, other than thrombin, have been identified, including other coagulation and fibrinolytic proteases. We have yet to explore potential PAR1 related mechanisms of immune evasion resulting from alternative means of activation, such as biased signaling induced by activated protein C (APC)-mediated PAR1 cleavage [59]. We did analyze potential effects of APC (and plasmin) stimulation on HHC-I cell surface expression but observed no effects. Given that APC-PAR1 directs a downstream pathway distinct from that engaged by thrombin-PAR1 [60], it is conceivable that APC-PAR1 signaling could account for some of the observed effects not fully accounted for by the thrombin pathway. In addition, plasmin has been identified as an agonist for PAR1 [61]. In preliminary studies we found that KPC tumor growth is significantly reduced in plasminogen-deficient mice (data not shown). Whether such a reduction in KPC tumor formation is linked to PAR1 signaling remains to be defined. Additionally, the nature of gene expression changes that APC-PAR1 or plasmin-PAR1 signaling can exert on KPC PDAC also remains an open question that we are actively investigating.

Collectively, our results further characterize a novel role for PAR1 in PDAC immune evasion, exploring the link between the coagulation pathway, inflammation, and tumor growth. PAR1 expression by tumor cells can influence tumor immune infiltration in part by driving expression of immunosuppressive factors critical for PDAC tumor growth. While this work has focused primarily on the involvement of cytotoxic T cells in anti-tumor immunity, our previous findings indicate that other immune cell populations also likely contribute to elimination of $PAR1^{KO}$ tumor cells [22], an area that will require further investigation. Given the poor immunogenicity of PDAC tumors it is critical to identify novel factors, such as PAR1, that impact the tumor/immune interface. Uncovering the interplay between coagulation signaling mechanisms and PDAC tumor immunity, can potentially point the way to developing novel immunotherapeutic strategies to target pancreatic cancer.

Supplementary Material

Refer to Web version on PubMed Central for supplementary material.

Acknowledgments

We would like to acknowledge the Bindley Bioscience Center's flow cytometry and cell separation facility for providing guidance and equipment for this study. The results shown here are in part based on data generated by the TCGA Research Network: http://www.cancer.gov/tcga.

Funding

This work was supported by grants to M.J. Flick (NIH R01CA211098: NIH U01HL143403) and S.F. Konieczny (NIH R01CA211098, NIH R01CA124586). The authors gratefully acknowledge support from the Purdue University Center for Cancer Research, NIH Grant No. P30 CA023168.

References

1. American Cancer Society. ACS cancer facts and figures. American Cancer Society 2019.
2. Khorana AA, Francis CW, Culakova E, Kuderer NM, Lyman GH. Frequency, risk factors, and trends for venous thromboembolism among hospitalized cancer patients. Cancer. 2007 11;110:2339–46. [PubMed: 17918266]
3. Cronin-Fenton DP, Søndergaard F, Pedersen LA, Fryzek JP, Cetin K, Acquavella J, et al. Hospitalisation for venous thromboembolism in cancer patients and the general population: A population-based cohort study in Denmark, 1997–2006. Br J Cancer. 2010 9;103:947–53. [PubMed: 20842120]
4. Cohen AT, Katholing A, Rietbrock S, Luke Bamber;, Carlos Martinez ; Epidemiology of first and recurrent venous thromboembolism in patients with active cancer A population-based cohort study. 2017;
5. Clark CE, Hingorani SR, Mick R, Combs C, Tuveson DA, Vonderheide RH. Dynamics of the immune reaction to pancreatic cancer from inception to invasion. Cancer Res. 2007 10;67:9518–27. [PubMed: 17909062]
6. Evans RA, Diamond MS, Rech AJ, Chao T, Richardson MW, Lin JH, et al. Lack of immunoediting in murine pancreatic cancer reversed with neoantigen. JCI Insight. 2016 9;1.
7. Fukunaga A, Miyamoto M, Cho Y, Murakami S, Kawarada Y, Oshikiri T, et al. CD8+tumor-infiltrating lymphocytes together with CD4+tumor-infiltrating lymphocytes and dendritic cells improve the prognosis of patients with pancreatic adenocarcinoma. Pancreas. 2004;28. [PubMed: 15211108]
8. Kabacaoglu D, Ciecielski KJ, Ruess DA, Algül H. Immune checkpoint inhibition for pancreatic ductal adenocarcinoma: Current limitations and future options Vol. 9, Frontiers in Immunology. Frontiers Media S.A.; 2018.
9. Sharma BK, Flick MJ, Palumbo JS. Cancer-Associated Thrombosis : A Two-Way Street. Semin Thromb Hemost. 2019;45:559–68. [PubMed: 31382306]
10. Soh UJ, Dores MR, Chen B, Trejo J. Signal transduction by protease-activated receptors. Vol. 160, British Journal of Pharmacology. 2010 p. 191–203. [PubMed: 20423334]
11. Heuberger DM, Schuepbach RA. Protease-activated receptors (PARs): mechanisms of action and potential therapeutic modulators in PAR-driven inflammatory diseases. Thromb J. 2019 12;17:4. [PubMed: 30976204]
12. Ossovskaya VS, Bunnett NW. Protease-Activated Receptors: Contribution to Physiology and Disease. Physiol Rev. 2004;84:579–621. [PubMed: 15044683]
13. Steinhoff M, Buddenkotte J, Shpacovitch V, Rattenholl A, Moormann C, Vergnolle N, et al. Proteinase-activated receptors: Transducers of proteinase-mediated signaling in inflammation and immune response. Endocr Rev. 2005;26:1–43. [PubMed: 15689571]
14. Adams GN, Sharma BK, Rosenfeldt L, Frederick M, Flick MJ, Witte DP, et al. Protease-activated receptor-1 impedes prostate and intestinal tumor progression in mice. J Thromb Haemost. 2018 11;16:2258–69. [PubMed: 30152921]
15. Goyama S, Shrestha M, Schibler J, Rosenfeldt L, Miller W, O'Brien E, et al. Protease-Activated Receptor 1 (PAR-1) Inhibits Proliferation but Enhances Leukemia Stem Cell Activity in Acute Myeloid Leukemia. Blood. 2016;
16. Boire A, Covic L, Agarwal A, Jacques S, Sherifi S, Kuliopulos A. PAR1 is a matrix metalloprotease-1 receptor that promotes invasion and tumorigenesis of breast cancer cells. Cell. 2005;120:303–13. [PubMed: 15707890]
17. Yang E, Boire A, Agarwal A, Nguyen N, O'Callaghan K, Tu P, et al. Blockade of PAR1 signaling with cell-penetrating pepducins inhibits Akt survival pathways in breast cancer cells and suppresses tumor survival and metastasis. Cancer Res. 2009;69:6223–31. [PubMed: 19622769]
18. Tantivejkul K, Loberg RD, Mawocha SC, Day LL, St. John L, Pienta BA, et al. PAR1-mediated NFκB activation promotes survival of prostate cancer cells through a Bcl-xL-dependent mechanism. J Cell Biochem. 2005;96:641–52. [PubMed: 16052512]

19. Adams GN, Rosenfeldt L, Frederick M, Miller W, Waltz D, Kombrinck K, et al. Colon cancer growth and dissemination relies upon thrombin, Stromal PAR-1, and fibrinogen. Cancer Res. 2015;75:4235–43. [PubMed: 26238780]
20. Fujimoto D, Hirono Y, Goi T, Katayama K, Matsukawa S, Yamaguchi A. The activation of proteinase-activated receptor-1 (PAR1) promotes gastric cancer cell alteration of cellular morphology related to cell motility and invasion. Int J Oncol. 2013 2;42:565–73. [PubMed: 23242308]
21. Yang E, Cisowski J, Nguyen N, O'Callaghan K, Xu J, Agarwal A, et al. Dysregulated protease activated receptor 1 (PAR1) promotes metastatic phenotype in breast cancer through HMGA2. Oncogene. 2016;35:1529–40. [PubMed: 26165842]
22. Yang Y, Stang A, Schweickert PG, Lanman NA, Paul EN, Monia BP, et al. Thrombin signaling promotes pancreatic adenocarcinoma through PAR-1–dependent immune evasion. Cancer Res. 2019;79:3417–30. [PubMed: 31048498]
23. Weber K, Bartsch U, Stocking C, Fehse B. A multicolor panel of novel lentiviral "gene ontology" (LeGO) vectors for functional gene analysis. Mol Ther. 2008;16:698–706. [PubMed: 18362927]
24. Tsai SQ, Wyvekens N, Khayter C, Foden J a, Thapar V, Reyon D, et al. Dimeric CRISPR RNA-guided FokI nucleases for highly specific genome editing. Nat Biotechnol. 2014 6;32:569–76. [PubMed: 24770325]
25. Zhu X, Xu Y, Yu S, Lu L, Ding M, Cheng J, et al. An efficient genotyping method for genome-modified animals and human cells generated with CRISPR/Cas9 system. Sci Rep. 2014 Sep;4:1–8.
26. Damiano BP, Cheung WM, Santulli RJ, Fung-Leung WP, Ngo K, Ye RD, et al. Cardiovascular responses mediated by protease-activated receptor-2 (PAR- 2) and thrombin receptor (PAR-1) are distinguished in mice deficient in PAR- 2 or PAR-1. J Pharmacol Exp Ther. 1999;
27. Pasut A, Oleynik P, Rudnicki MA. Isolation of muscle stem cells by fluorescence activated cell sorting cytometry. Methods Mol Biol. 2012;798:53–64. [PubMed: 22130830]
28. Uhlén M, Fagerberg L, Hallström BM, Lindskog C, Oksvold P, Mardinoglu A, et al. Tissue-based map of the human proteome. Science (80-). 2015 1;347.
29. Chen Y, Song Y, Du W, Gong L, Chang H, Zou Z. Tumor-associated macrophages: An accomplice in solid tumor progression Vol. 26, Journal of Biomedical Science. BioMed Central Ltd; 2019 p. 1–13. [PubMed: 30602371]
30. Gabrilovich DI. Myeloid-derived suppressor cells. Cancer Immunol Res. 2017 1;5:3–8. [PubMed: 28052991]
31. Garcia-Lora A, Algarra I, Garrido F. MHC class I antigens, immune surveillance, and tumor immune escape. J Cell Physiol. 2003 6;195:346–55. [PubMed: 12704644]
32. Doody GM, Stephenson S, McManamy C, Tooze RM. PRDM1/BLIMP-1 Modulates IFN-γ-Dependent Control of the MHC Class I Antigen-Processing and Peptide-Loading Pathway. J Immunol. 2007 12;179:7614–23. [PubMed: 18025207]
33. Johnsen AK, Templeton DJ, Sy M, Harding CV. Deficiency of transporter for antigen presentation (TAP) in tumor cells allows evasion of immune surveillance and increases tumorigenesis. J Immunol. 1999;
34. Wei SC, Duffy CR, Allison JP. Fundamental mechanisms of immune checkpoint blockade therapy Vol. 8, Cancer Discovery. American Association for Cancer Research Inc.; 2018 p. 1069–86. [PubMed: 30115704]
35. Hornyák L, Dobos N, Koncz G, Karányi Z, Páll D, Szabó Z, et al. The role of indoleamine-2,3-dioxygenase in cancer development, diagnostics, and therapy Vol. 9, Frontiers in Immunology. Frontiers Media S.A.; 2018.
36. Peter ME, Hadji A, Murmann AE, Brockway S, Putzbach W, Pattanayak A, et al. The role of CD95 and CD95 ligand in cancer Vol. 22, Cell Death and Differentiation. Nature Publishing Group; 2015 p. 549–59. [PubMed: 25656654]
37. Nakasone Y, Fujimoto M, Matsushita T, Hamaguchi Y, Huu D Le, Yanaba M, et al. Host-derived MCP-1 and MIP-1α regulate protective anti-tumor immunity to localized and metastatic B16 melanoma. Am J Pathol. 2012 1;180:365–74. [PubMed: 22037251]

38. Zelenay S, van der Veen GA, Bottcher PJ, Snelgrove JK, Rogers N, Acton ES, et al. Cyclooxygenase-Dependent Tumor Growth through Evasion of Immunity. Cell. 2015;1257–70. [PubMed: 26343581]
39. Markosyan N, Li J, Sun YH, Richman LP, Lin JH, Yan F, et al. Tumor cell-intrinsic EPHA2 suppresses antitumor immunity by regulating PTGS2 (COX-2). J Clin Invest. 2019 9;129:3594–609. [PubMed: 31162144]
40. Bayne LJ, Beatty GL, Jhala N, Clark CE, Rhim AD, Stanger BZ, et al. Tumor-derived granulocyte-macrophage colony-stimulating factor regulates myeloid inflammation and T cell immunity in pancreatic cancer. Cancer Cell. 2012 6;21:822–35. [PubMed: 22698406]
41. Pylayeva-Gupta Y, Lee KE, Hajdu CH, Miller G, Bar-Sagi D. Oncogenic Kras-induced GM-CSF production promotes the development of pancreatic neoplasia. Cancer Cell. 2012 6;21:836–47. [PubMed: 22698407]
42. Wang J, Sun J, Liu LN, Flies DB, Nie X, Toki M, et al. Siglec-15 as an immune suppressor and potential target for normalization cancer immunotherapy. Nat Med. 2019 4;25:656–66. [PubMed: 30833750]
43. Baghdadi M, Wada H, Nakanishi S, Abe H, Han N, Putra WE, et al. Chemotherapy-Induced IL34 Enhances Immunosuppression by Tumor-Associated Macrophages and Mediates Survival of Chemoresistant Lung Cancer Cells. 2016;
44. Hargadon K Dysregulation of TGFβ1 Activity in Cancer and Its Influence on the Quality of Anti-Tumor Immunity. J Clin Med. 2016 8;5:76.
45. Bronte V, Chappell DB, Apolloni E, Cabrelle A, Wang M, Hwu P, et al. Unopposed production of granulocyte-macrophage colony-stimulating factor by tumors inhibits CD8+ T cell responses by dysregulating antigen-presenting cell maturation. J Immunol. 1999 5;162:5728–37. [PubMed: 10229805]
46. Sotomayor EM, Fu YX, Lopez-Cepero M, Herbert L, Jimenez JJ, Albarracin C, et al. Role of tumor-derived cytokines on the immune system of mice bearing a mammary adenocarcinoma. II. Down-regulation of macrophage-mediated cytotoxicity by tumor-derived granulocyte-macrophage colony-stimulating factor. J Immunol. 1991 10;147:2816–23. [PubMed: 1918995]
47. Frossard JL, Saluja AK, Mach N, Lee HS, Bhagat L, Hadenque A, et al. In vivo evidence for the role of GM-CSF as a mediator in acute pancreatitis-associated lung injury. Am J Physiol - Lung Cell Mol Physiol. 2002 9;283:L541–8. [PubMed: 12169573]
48. Lang RA, Metcalf D, Cuthbertson RA, Lyons I, Stanley E, Kelso A, et al. Transgenic mice expressing a hemopoietic growth factor gene (GM-CSF) develop accumulations of macrophages, blindness, and a fatal syndrome of tissue damage. Cell. 1987 11;51:675–86. [PubMed: 3499986]
49. Weinstein JR, Zhang M, Kutlubaev M, Lee R, Bishop C, Andersen H, et al. Thrombin-induced regulation of CD95(Fas) expression in the N9 microglial cell line: Evidence for involvement of proteinase-activated receptor1 and extracellular signal-regulated kinase 1/2. Neurochem Res. 2009 3;34:445–52. [PubMed: 18686031]
50. Colognato R, Slupsky JR, Jendrach M, Burysek L, Syrovets T, Simmet T. Differential expression and regulation of protease-activated receptors in human peripheral monocytes and monocyte-derived antigen-presenting cells. Blood. 2003 10;102:2645–52. [PubMed: 12805069]
51. Chen D, Carpenter A, Abrahams J, Chambers RC, Lechler RI, McVey JH, et al. Protease-activated receptor 1 activation is necessary for monocyte chemoattractant protein 1-dependent leukocyte recruitment in vivo. J Exp Med. 2008 8;205:1739–46. [PubMed: 18606855]
52. Chien PTY, Hsieh HL, Chi PL, Yang CM. PAR1-dependent COX-2/PGE2 production contributes to cell proliferation via EP2 receptors in primary human cardiomyocytes. Br J Pharmacol. 2014 10;171:4504–19. [PubMed: 24902855]
53. Houliston RA, Keogh RJ, Sugden D, Dudhia J, Carter TD, Wheeler-Jones CPD. Protease-activated receptors upregulate cyclooxygenase-2 expression in human endothelial cells. Thromb Haemost. 2002;88:321–8. [PubMed: 12195707]
54. Peters T, Henry PJ. Protease-activated receptors and prostaglandins in inflammatory lung disease Vol. 158, British Journal of Pharmacology. Wiley-Blackwell; 2009 p. 1017–33. [PubMed: 19845685]

55. Wakita H, Furukawa F, Takigawa M. Thrombin and trypsin induce granulocyte-macrophage colony-stimulating factor and interleukin-6 gene expression in cultured normal human keratinocytes. Proc Assoc Am Physicians. 1997 3;109:190–207. [PubMed: 9069588]

56. Shimaya Y, Shimada M, Shutto Y, Fujita T, Murakami R, Nakamura N, et al. Thrombin Stimulates Synthesis of Macrophage Colony-Stimulating Factor, Granulocyte-Macrophage Colony-Stimulating Factor and Granulocyte Colony-Stimulating Factor by Human Proximal Tubular Epithelial Cells in Culture. Nephron Extra. 2012 1;2:1–8. [PubMed: 22479263]

57. Ungefroren H, Gieseler F, Kaufmann R, Settmacher U, Lehnert H, Rauch BH. Signaling crosstalk of TGF-β/ALK5 and PAR2/PAR1: A complex regulatory network controlling fibrosis and cancer. Vol. 19, International Journal of Molecular Sciences. MDPI AG; 2018.

58. Wang M, Zhao J, Zhang L, Lian Y, Wu Y, Gong Z, et al. Role of tumor microenvironment in tumorigenesis. J Cancer. 2017;8:761–73. [PubMed: 28382138]

59. Zhao P, Metcalf M, Bunnett NW. Biased signaling of protease-activated receptors Vol. 5, Frontiers in Endocrinology. Frontiers Media S.A.; 2014.

60. Mosnier LO, Sinha RK, Burnier L, Bouwens EA, Griffin JH. Biased agonism of protease-activated receptor 1 by activated protein C caused by noncanonical cleavage at Arg46. Blood. 2012 12;120:5237–46. [PubMed: 23149848]

61. Kuliopulos A, Covic L, Seeley SK, Sheridan PJ, Helin J, Costello CE. Plasmin desensitization of the PAR1 thrombin receptor: Kinetics, sites of truncation, and implications for thrombolytic therapy. Biochemistry. 1999 4;38:4572–85. [PubMed: 10194379]

Essentials

- Elimination of PDAC tumor cell PAR1 increased cytotoxic T cells and reduced tumor macrophages.
- $PAR1^{KO}$ PDAC cells are preferentially eliminated from growing tumors.
- Thrombin-PAR1 signaling in PDAC tumor cells drives an immunosuppressive gene signature.
- *Csf2* and *Ptgs2* are thrombin-PAR1 downstream immun suppressor genes in PDAC tumor cells.

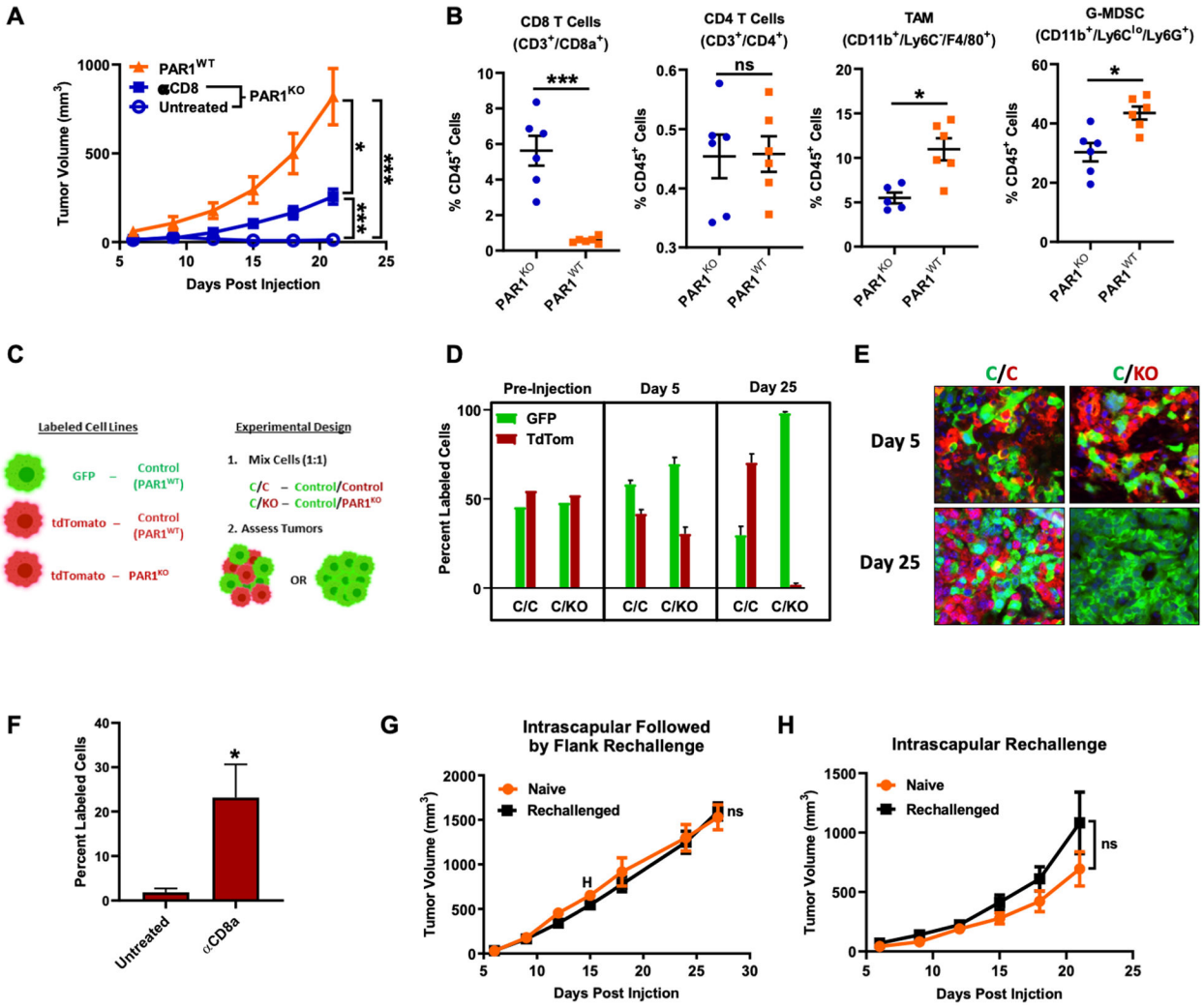

Figure 1: PAR1^{KO} tumor cells display an increased anti-tumor immune response and are more susceptible to immune cell targeting and elimination.

(A) Subcutaneous (s.c.) tumor growth of KPC cells in C57BL/6 mice with or without treatment with CD8a targeting monoclonal antibodies (αCD8) (n = 6–9 mice/group). (B) Analysis of various immune infiltrates in s.c. tumors 9-days post injection based on the indicated cell surface markers. (C) Experimental design for the PAR1^{WT}/PAR1^{KO} mixed tumor experiments. (D) Quantification of fluorescently labeled PAR1^{WT} and PAR1^{KO} cells prior to injection and from dissociated tumors at the indicated time points (n = 6 tumors/group). (E) Representative immunofluorescence images of the tumor samples quantified in (D). (F) Quantification of PAR1^{KO} tumor cells in PAR1^{WT}/PAR1^{KO} mixed tumors with or without αCD8a treatment harvested 25 days post injection. Bars represent PAR1^{KO} cells as a percent of total labeled tumor cells (n = 6 mice/group). (G and H) Tumor growth from C57BL/6 tumor rechallenge studies. Mice were initially injected in the intrascapular region with PAR1^{KO} cells and tumors were allowed to fully regress for 36 days before the mice were rechallenged with PAR1^{WT} cells in either the flank or intrascapular region. Naïve littermate mice that received no initial PAR1^{WT} injection were used for comparison (n = 4–8 mice/group). Error bars represent SEM. *P< 0.05 by Student's T test.

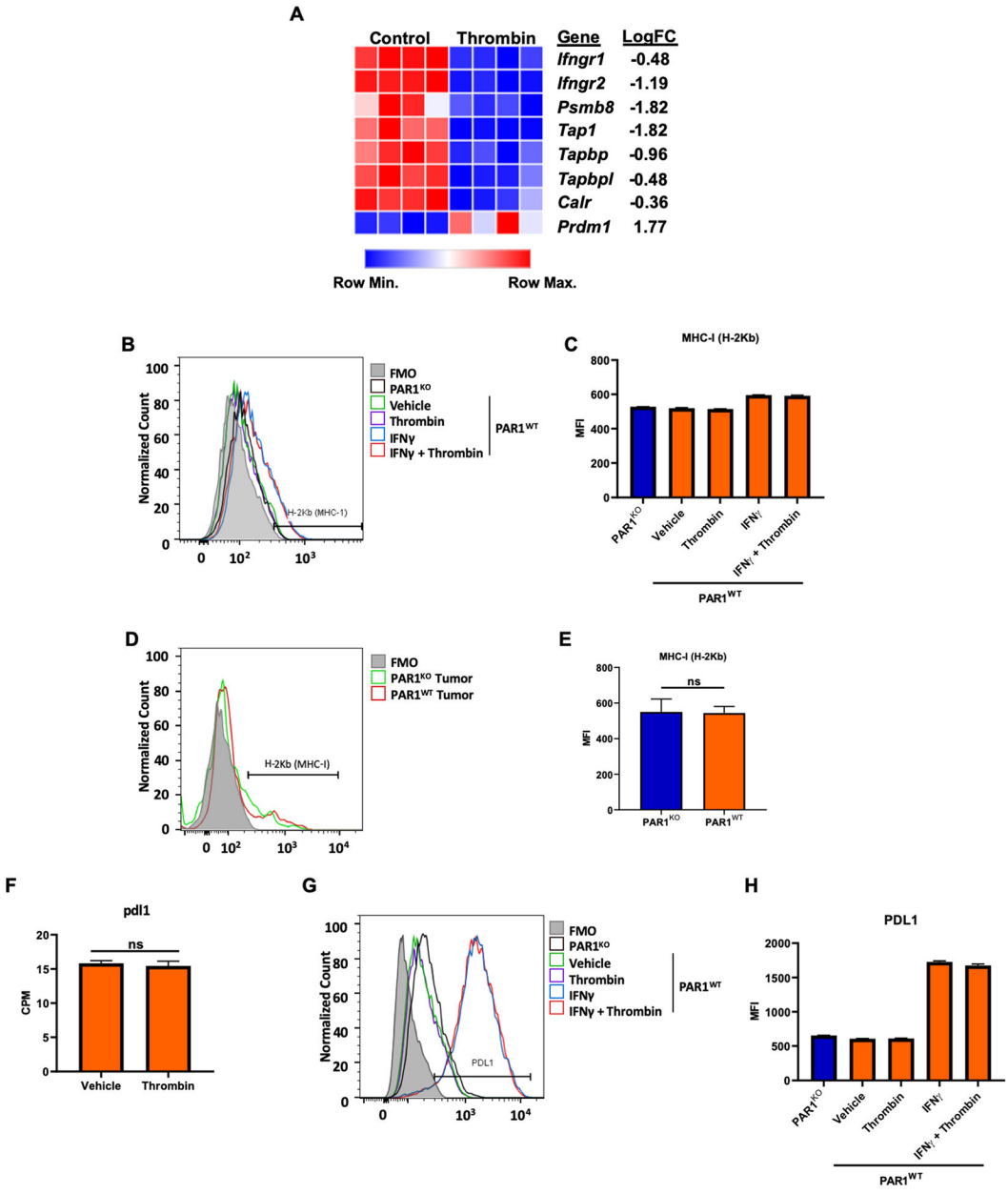

Figure 2: PAR1 signaling does not affect MHC-I or PDL1 protein expression.

(A) Heatmap showing relative expression levels of various gene targets related to antigen processing and MHC-I loading from the RNA-Seq analysis, FDR < 0.01 for all genes listed. (B) Representative histograms and (C) quantification of MHC-I molecule H-2Kb expression for KPC-PAR1^{KO} cells and KPC-PAR1^{WT} cells following treatment with vehicle, thrombin, IFNγ or IFNγ and thrombin. Samples were harvested 48 hours after thrombin exposure and 24 hours after treatment with IFNγ. (n = 3/group). (D) Representative histogram and (E) quantification of H-2Kb expression on PAR1^{WT} and PAR1^{KO} cells harvested 7-days post injection from tumors recovered from C57Bl/6 mice. Both cell lines expressed tdTomato for identification by flow cytometry (n = 3/group). (F) Expression of *pdl1* based on the RNA-Seq analysis represented as counts per million (CPM). (G) Representative flow cytometry

results for PDL1 in $PAR1^{WT}$ cells under various treatment conditions (n = 3/group). (H) Quantification of the results depicted in (G). For (C) and (H). FMO - fluorescence minus one, MFI - median fluorescence intensity. Error bars represent SEM. ns – not significant.

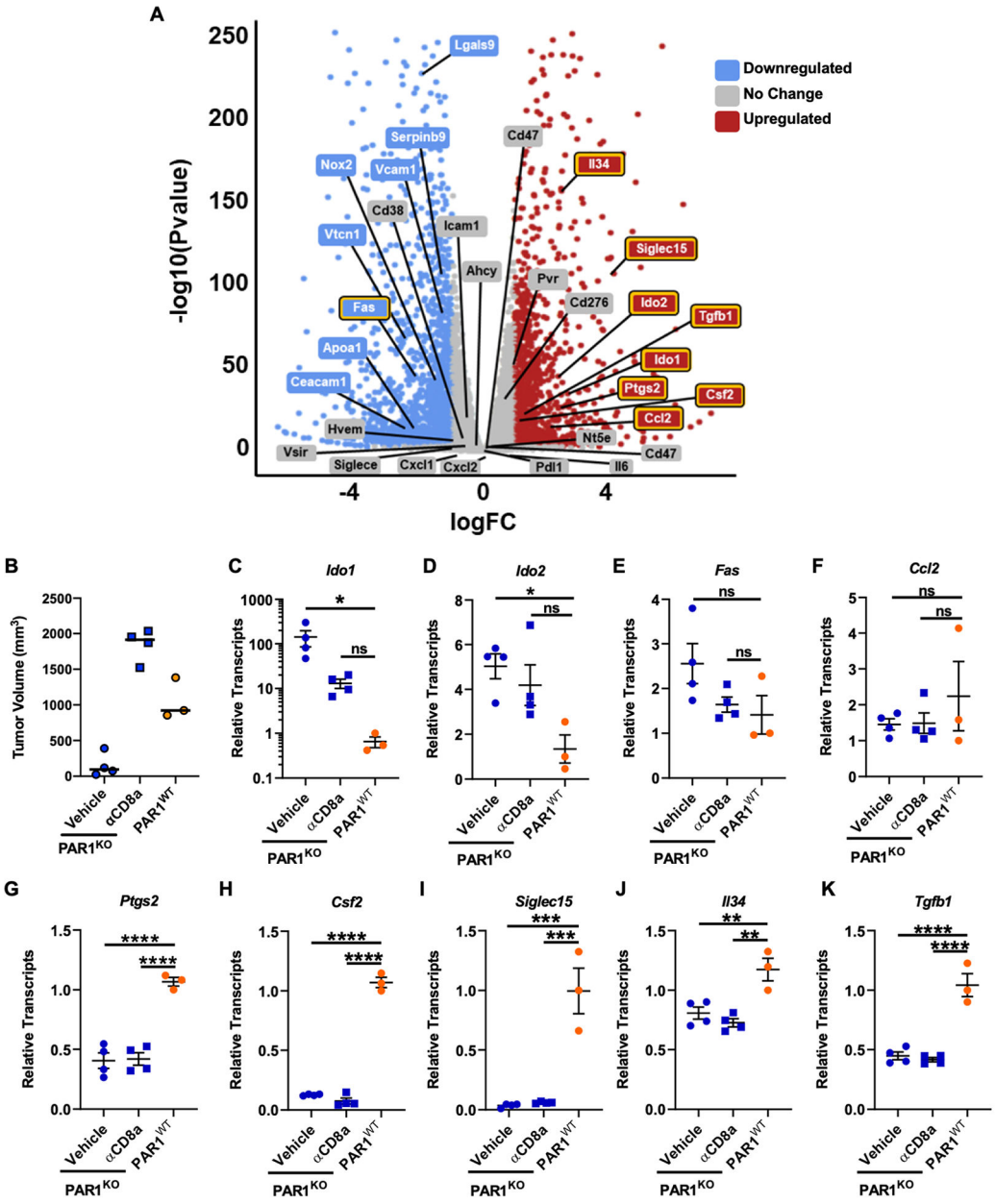

Figure 3: PAR1 signaling induces expression of immunosuppressive genes.

(A) Volcano plot depicting the RNA-Seq results from PAR1^{WT} cells treated with or without thrombin for 24 h. Specific genes related to immunosuppression are highlighted. Note that the following genes were also analyzed but had no detectable transcripts: *Pdl2, Cd80, Cd86, Tdo, Cd200, FasL, Cd39*, and *Pap*. Differential expression was defined as FDR ≤ 0.01, fold-change ≥ 2. (B) Final tumor volume for the samples used to analyze PAR1 downstream target expression *in vivo*, note that PAR1^{KO} tumors from αCD8a treated mice in this study were allowed to progress until they reached equal or greater size than the PAR1^{WT} control samples in order to eliminated tumor size as a confounding factor in the analysis. (C-K) RT-qPCR results assessing the relative expression of various genes in whole RNA samples from

the indicated tumor conditions. Results were normalized to *Actb* expression and analyzed using Dunnett's post hoc test. * $P < 0.05$, ** $P < 0.01$, *** $P < 0.001$, **** $P < 0.0001$.

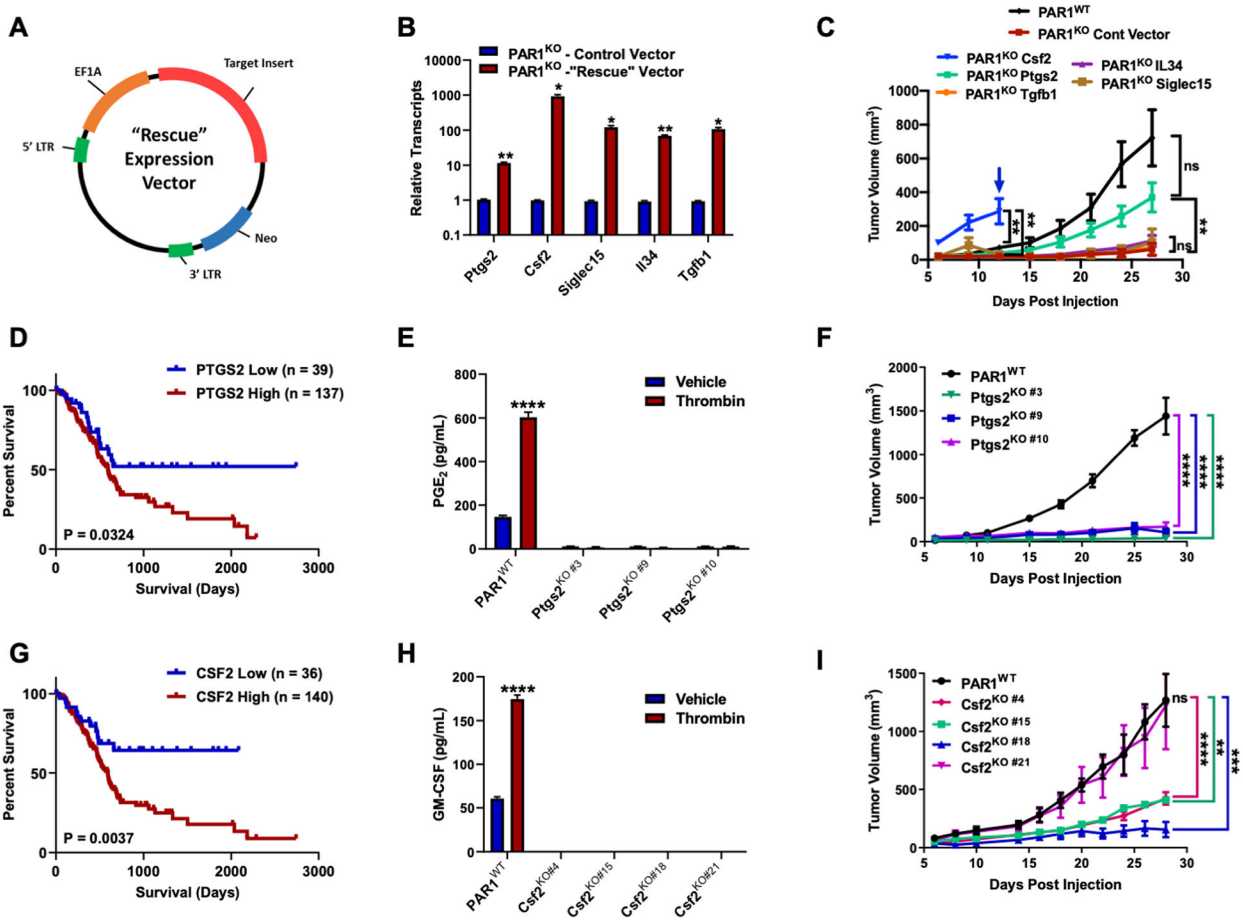

Figure 4: PAR1 signaling induces expression of *Ptgs2* and *Csf2*, both of which are critical for PDAC tumor growth.

(A) Generalized map of the lentiviral vector used to introduce PAR1 downstream targets into the PAR1^{KO} cell line. (B) RT-qPCR confirmation of the ectopically expressed "rescue" cell lines. (C) Analysis of the s.c. tumor growth of the various PAR1^{KO} overexpression (OE) rescue cell lines. Note the PAR1^{KO} CSF2-OE group was terminated early due to health concerns as indicated by the blue arrow (n = 7–9 mice/group). (D and G) Kaplan-Meier survival plots based on TCGA PDAC patient data; significance was calculated using a log-rank test. (E and H) ELISA results using conditioned media harvested 48 hours after thrombin or vehicle treatment (n = 3/group). (F and I) Analysis of s.c. tumor growth of the indicated cell lines (n = 4–8 mice/group). * $P < 0.05$, ** $P < 0.01$, *** $P < 0.001$, **** $P < 0.0001$, ns – not significant.